Available online at www.sciencedirect.com
ScienceDirect
Trans. Nonferrous Met. Soc. China 26(2016) 3070−3080
Transactions of Nonferrous Metals Society of China
www.tnmsc.cn

Microstructure evolution and mechanical properties of rheo-processed ADC12 alloy

Zhao-hua HU, Xiang PENG, Guo-hua WU, Da-qiang CHENG, Wen-cai LIU, Liang ZHANG, Wen-jiang DING

National Engineering Research Center of Light Alloys Net Forming and State Key Laboratory of Metal Matrix Composite, Shanghai Jiao Tong University, 200240 Shanghai, China

Received 8 September 2016; accepted 10 November 2016

Abstract: Microstructure evolution and mechanical properties of the rheo-processed ADC12 alloy were investigated by means of optical microscopy, X-ray diffraction and scanning electron microscopy. Primary dendritic Al of rheo-casting (RC) and rheo-diecasting (RDC) ADC12 alloys are sheared off. The average size, as well as solid fraction of the primary Al increase with descending pouring temperature. The mechanical properties of alloys are strengthened by rheo-processing. Ultimate tensile strengths of RC samples increase with the decrease of the pouring temperature, and reach the maximum in the range from 580 to 600 °C. At pouring temperature of 595 °C, the RDC sample obtains the best ultimate tensile strength and elongation. Great reductions on porosity and primary Al globularization are crucial to the mechanical properties. Relationships of the primary Al size and yield stress are depicted with Hall−Petch equation.

Key words: aluminum alloy; casting; rheo-processing; rheo-casting; rheo-diecasting; mechanical properties

1 Introduction

In the past decades, the replacement of iron and steel by aluminum in automotive industry has been increasing due to its contribution to mass reduction and lower gas emission [1,2]. As one kind of Al−Si alloys, the ADC12 aluminum alloy is extensively used in automobile based on its high castability, high productivity, low shrinkage rate and relatively good corrosion resistance [3,4].

Rheo-processing is a branch of semi-solid processing (SSP), which requires the liquid metal alloy to be cooled between the liquidus and solidus temperatures with some forms of agitation and then being high pressure die cast or permanent mold cast, resulting in a globular or spherical primary solid microstructure. The rheo-processing exhibits significant advantages over the traditional material processing techniques, such as good net shape capability, low energy cost, less entrapped air, fine grain size, reduction in solidification shrinkage, porosity and segregation, and has been widely accepted [5,6].

The ADC12 alloy, whose silicon content is close to the eutectic point in the Al−Si binary equilibrium phase diagram, is considered not suitable for rheo-processing because of its narrow liquidus−solidus region. To date, few research efforts about rheo-processing of the ADC12 alloy are reported. WANG et al [7] adopted a thixo-processing way called SIMA method to produce semisolid ADC12 alloy, and the spherical primary Al was obtained but in a large diameter over 100 μm. JANUDOM et al [8] used the gas induced semisolid (GISS) method successfully produced ADC12 semisolid die casting aluminum alloy, and they tried to prepare the rheo-extruded ADC12 alloy with the same method but fail to obtain the ideal spherical primary phase [9]. However, none of them referred to the rheo-processed mechanical properties.

In our previous work [10], it was proved that the dendritic primary Al of ADC12 alloy could be sheared off by strong shearing forces and hence the spherical primary phase was successfully obtained by means of mechanical rotational barrel (MRB) system. In this work, the microstructural evolution of the ADC12 alloy rheo-processed by the MRB system, and then being subjected to rheo-casting (RC) and rheo-diecasting (RDC) was investigated. The aim of this work is to establish the

Foundation item: Project (51404153) supported by the National Natural Science Foundation of China
Corresponding author: Guo-hua WU; Tel: +86-21-54742630; Fax: +86-21-34202794; E-mail: ghwu@sjtu.edu.cn
DOI: 10.1016/S1003-6326(16)64439-4

correlationship between processing parameters and mechanical properties, and finally promote the eutectic series alloy's rheo-processing and application.

2 Experimental

2.1 Principle of the MRB system

The principle of MRB system for rheo-casting and rheo-diecasting is shown in Fig. 1. The alloy used in this study was a commercial ADC12 alloy (Table 1). The sequence for rheo-forming of the ADC12 alloy was divided into two steps. First, semisolid slurry preparation, and then rheo-casting or high pressure die casting. The preparation of the semisolid slurry employed a mechanical rotational barrel (MRB) system. The barrel was made of stainless steel, with an inclination angle of 45°, and 500 mm in length and 150 mm in diameter. The alloy melt flow inside the barrel was characterized by high shear rate and turbulence. The basic function of the MRB system is to convert the alloy melt into high quality semisolid slurry by high shear rate and turbulence through solidification.

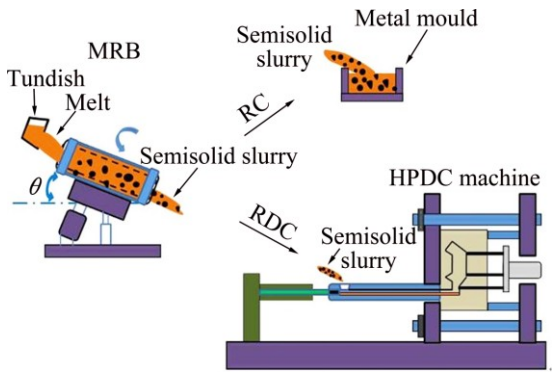

Fig. 1 Schematic diagram of MRB system for rheo-casting and rheo-diecasting

Table 1 Chemical composition of ADC12 alloy (mass fraction, %)

Si	Cu	Mn	Mg	Fe	Ni	Zn	Al
10.18	1.60	0.25	0.19	0.70	0.05	0.89	Bal.

2.2 Rheo-casting and Rheo-diecasting process

After being processed by the MRB system, the semisolid slurry was solidified in the permanent mould which was preheated to 200 °C. The temperatures of the alloy melt poured in the MRB system for subsequent rheo-casting were 580, 600 and 620 °C, and the barrel rotational speed was 60 r/min.

After slurry preparation, the traditional high pressure die casting (HPDC) machine was employed for the rheo-diecasting. In this study, the temperatures of the alloy melt poured in the MRB system for rheo-diecasting were 585, 595 and 605 °C, and the barrel rotational speed was 60 r/min.

2.3 Microstructure observation and mechanical property test

All microstructure specimens were prepared by the standard procedure, and etched in an erodent with compositions of 2% hydrofluoric acid (HF), 3% hydrochloric acid (HCl), 5% nitric acid (HNO_3) and the rest water. Microstructure examination was performed using a ZEISS Axio Observer A1 optical microscope (OM) with a quantitative image analysis system.

A Netzsch STA449F3 differential scanning calorimetry (DSC) was employed to determine solidification interval. 3 mm diameter disc samples weighing 5−10 mg were scanned between 450 and 650 °C at a speed of 2 °C/min in an argon atmosphere.

Phase investigations were carried out using X-ray diffraction (XRD) with Cu K_α radiation using a Rigaku D/Max-2500 V diffractometer. A Hitachi S−3400N scanning electron microscope (SEM) equipped with an energy-dispersive X-ray (EDX) spectrometer was used for microstructural observation, phase composition identification and fractured surfaces observation. The porosity analysis was followed the method shown in WANNASIN's work [8]. The room temperature tensile properties were tested on Zwick/Roell testing machine. The tensile specimens have a gauge length of 10 mm, a gauge width of 3.5 mm and thickness of 2 mm.

3 Results

3.1 Solidus−liquidus determination and phase analysis

From the preliminary observation of the commercial ADC12 alloy, the solidus−liquids temperature range was determined. Figure 2 presents the differential scanning calorimetry (DSC) thermogram of the ADC12 alloy. In the solidifying thermogram, only one large peak which has been widely known as Al−Si binary reaction is observed [11]. The reaction starts from 575 °C and peaks

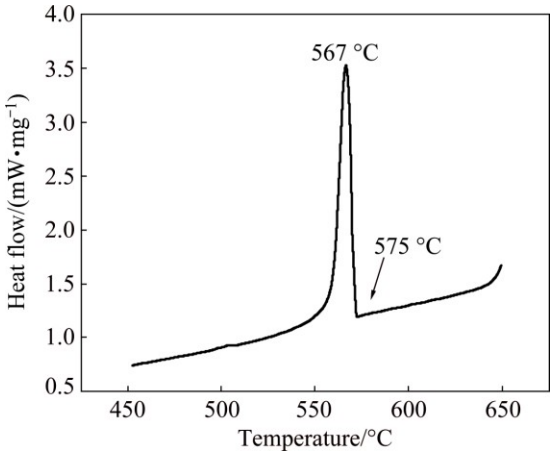

Fig. 2 Differential scanning calorimetry (DSC) thermogram of ADC12 alloy

at 567 °C, implying the obvious solidus−liquids temperature interval is about 10 °C.

The XRD patterns of the ADC12 alloy processed at different conditions are shown in Fig. 3. By conventional casting procedure without rheo-processing, the XRD patterns of the permanent mold casting (A_0) and high pressure die casting (B_0) show that it is mainly composed of three phases, which is Al, Si and Al_2Cu, respectively.

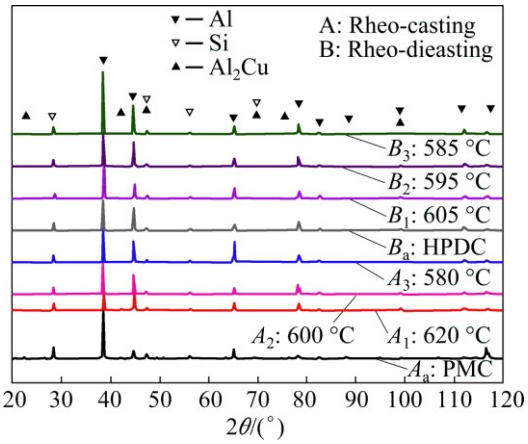

Fig. 3 XRD patterns of ADC12 alloy processed under different conditions

The RC samples rheo-processed at 620, 600, 580 °C (A_1, A_2, A_3) exhibit the same XRD patterns as liquid casting (A_0), and the reflections of the Al slightly shift towards to higher degree. Similarly, the XRD reflections of the Al phases in RDC ADC12 alloy processed at 605, 595, 585 °C (B_1, B_2, B_3) also present the higher degree movements. The higher degree movements of the Al reflections indicate that the solutions in the matrix decrease after rheo-processing, implying that the rheo-procesing has little effect on the solidification procedure.

3.2 Microstructural analysis

Figure 4 shows the microstructures of the liquid casting and rheo-casting ADC12 alloys at different pouring temperatures. The liquid casting ADC12 alloy exhibits typical microstructural features of Al−Si irregular eutectic solidification (as shown in Fig. 4(a)), some Al phases exist as primary dendrites with an average arm width of 81.6 μm, and the others solidify combining with Si in forms of irregular eutectic structure.

Table 2 shows the loss of temperature of ADC12 alloy for rheo-casting with different pouring temperatures. It is clear that the temperatures at the end of the barrel have greatly decreasing relationships versus pouring temperature and all of which are below the eutectic point comparing to the DSC thermogram (shown in Fig. 2), and with higher superheat, the higher cooling rate was obtained. Figure 5 presents the variation of solid fraction and primary Al average grain size of the rheo-casting ADC12 alloy obtained at different pouring temperatures. After rheo-processing, the primary

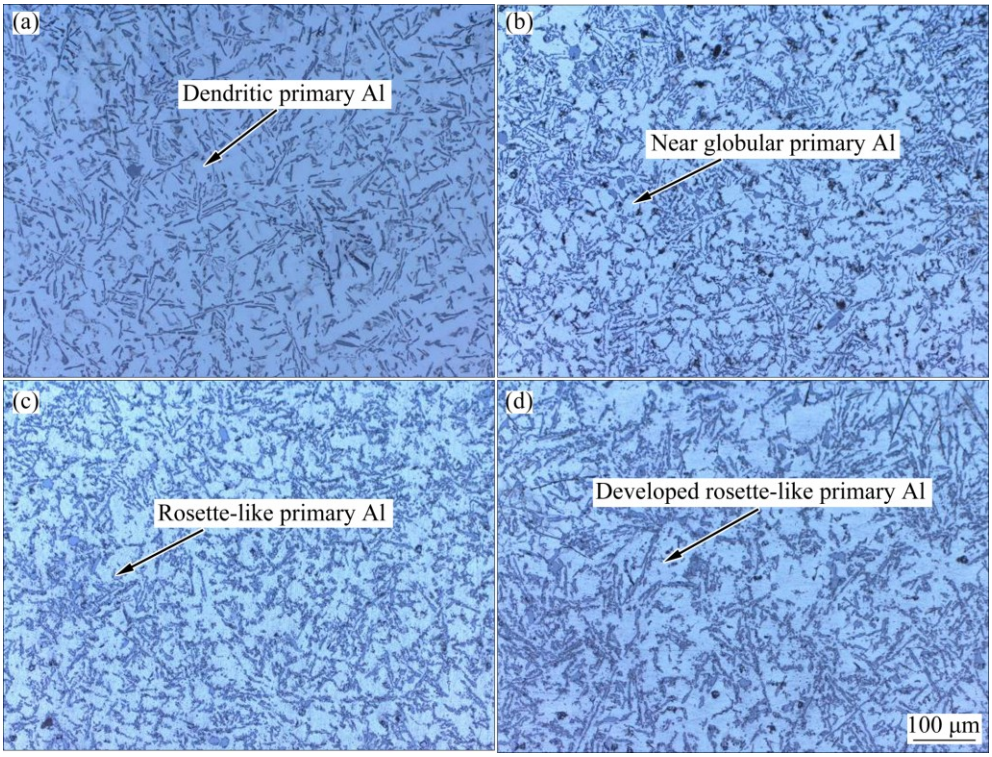

Fig. 4 Microstructures of liquid casting and rheo-casting ADC12 alloys processed at different pouring temperatures by permanent mold casting: (a) Liquid casting; (b) 620 °C; (c) 600 °C; (d) 580 °C

Table 2 Loss of temperature of ADC12 alloy for rheo-casting with different pouring temperatures

Pouring temperature/°C	Outlet temperature/°C	Temperature drop/°C	Cooling rate on barrel/(°C·s^{-1})
620	575	45	28.1
600	570	30	14.3
580	569	11	4.6

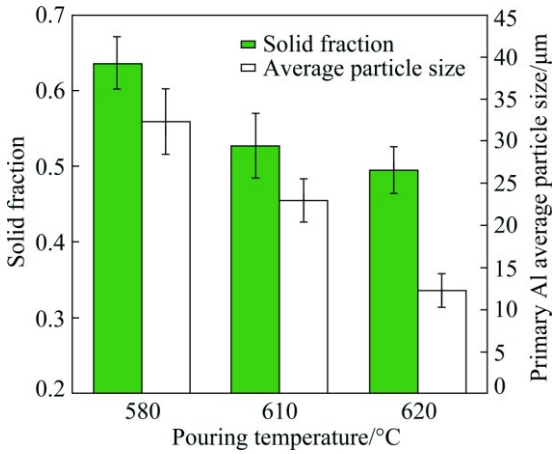

Fig. 5 Solid fraction and primary Al average particle size of rheo-casting ADC12 alloy at different pouring temperatures

dendrites are obviously sheared off, and ADC12 alloy shows a totally different microstructure. At the pouring temperature of 620 °C, it is observed that the primary Al exhibit nearly globular shape and distribute relatively uniformly in the matrix (shown in Fig. 4(b)). The primary α(Al) average grain size is about 27 μm, and the solid fraction is 0.33. As the pouring temperature decreases, the alloy presents a tendency that the shape of the primary phase transforms from near globular to rosette-like. At 600 °C, the primary Al particles mainly exist as equaixed shape and are obviously coarsened, and some of them are rosette-like. Their average grain size and solid fraction are 31 μm and 0.45, respectively. As for 580 °C, the rosette primary Al is further developed and rarely equaixed primary Al is observed, and average grain size and solid fraction of the rosette-like primary Al are increased to 39 μm and 0.56, respectively. Not only the primary phase, but also the eutectic Si is influenced by rheo-processing. The fraction of eutectic Si decreases as the pouring temperature drops. At 600 and 620 °C, the eutectic Si exhibits relatively fine acicular-like shape but changes to flake-like at 580 °C.

The liquid high pressure die casting (HPDC) and rheo-diecasting microstructures of the ADC12 alloy stirred with different pouring temperatures at a rotational speed of 60 r/min are shown in Fig. 6, and the corresponding outlet temperatures are presented in Table 3. The HPDC alloy shows typical dendritic growth morphology with long columnar dendrites observed in a matrix of fine eutectic. Similar to some hypoeutectic Al alloys, the ADC12 alloy exhibits a globular primary Al rheo-diecasting microstructure. As widely accepted, the RDC primary Al phase is divided into three categories [12]. The large spherical particle produced during the slurry period is named as α_1, the relatively small

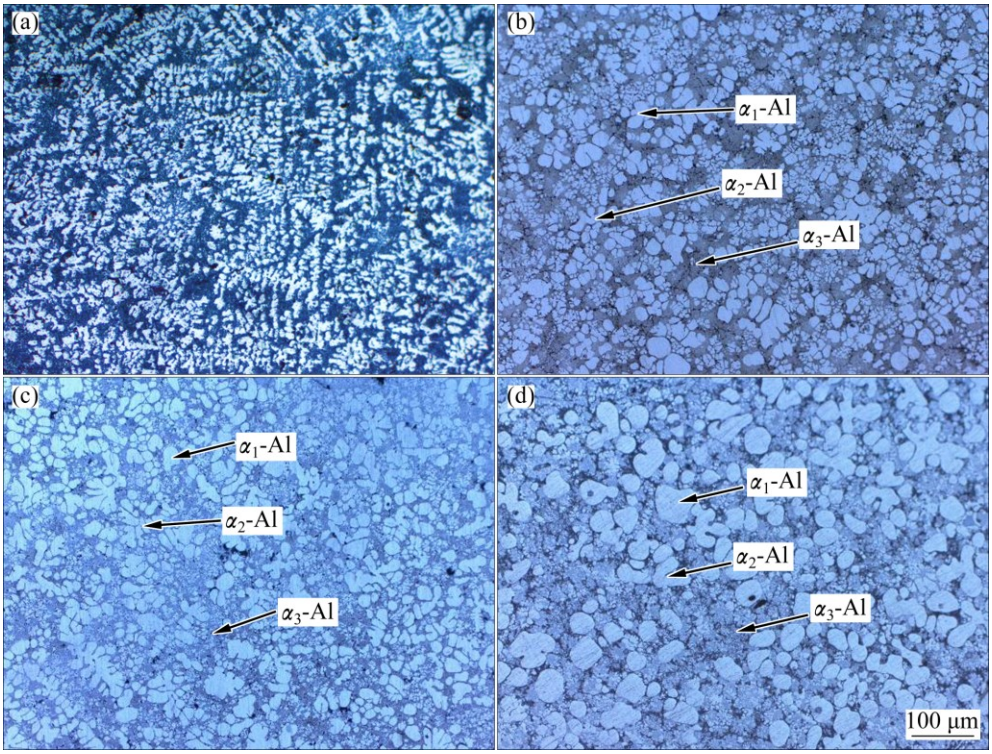

Fig. 6 Microstructures of ADC12 alloy by HPDC at pouring temperature of 620 °C (a) and RDC at pouring temperature of 605 °C (b), 595 °C (c) and 585 °C (d)

Table 3 Loss of temperature of ADC12 alloy for rheo-diecasting with different pouring temperatures

Pouring temperature/°C	Outlet temperature/°C	Temperature drop/°C	Cooling rate on barrel/(°C·s^{-1})
605	572	33	15.7
595	571	24	10.9
585	570	15	6.8

spherical particle solidified in the die cavity is marked as α_3, and the one during slurry transferring into the die in a dendritic growing is referred as α_2. By microstructure observation, there are abundant α_1 and α_3 after rheo-processing, while α_2 is rarely observed. Figure 7(a) presents the variation of solid fraction the rheo-diecasting ADC12 alloy obtained at different pouring temperatures. The RDC solid fraction is obviously increased with lowering pouring temperature, which is from 0.43 at 605 °C to 0.56 at 585 °C. The average sizes of α_1 and α_3 are plotted in Fig. 7(b) as functions of pouring temperature. The average size of α_1 remains nearly constant from 605 to 595 °C at around 26 μm, however, increases dramatically to 35 μm while poured at 585 °C. The abrupt increment of α_1 size is attributed to

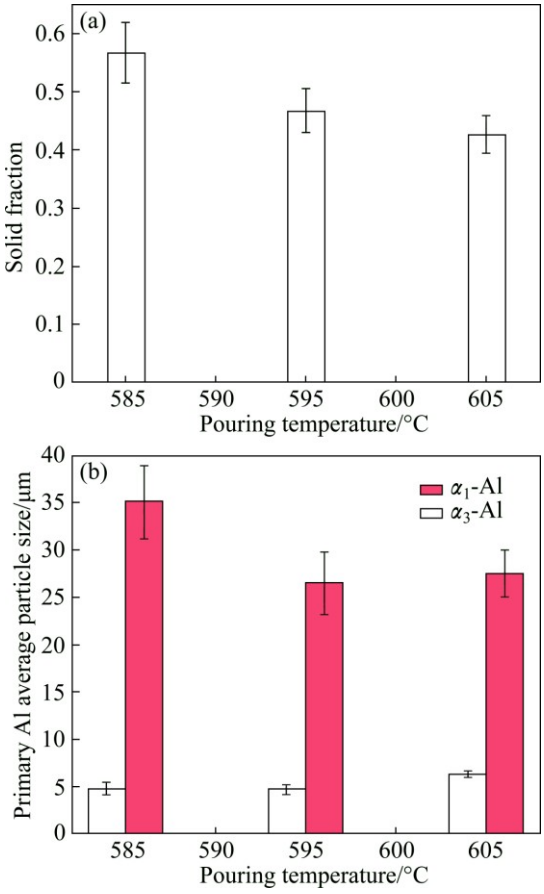

Fig. 7 Solid fraction (a) and primary Al average particle size (b) of rheo-diecasting ADC12 alloy at different pouring temperatures

the relatively slow cooling rate shown in Table 3. The plotted average size curve of α_3 is relatively smooth, and it decreases from 6.3 to 4.8 μm at temperatures from 605 to 585 °C, implying that it is not sensitively affected by pouring temperature. Further detailed microstructure observation carried out by SEM is presented in Fig. 8. The very fine α_3 particle is uniformly distributed in the matrix, clearly being sketched in the tiny lamellar eutectic Si which is also originated from the last solidification in the die cavity. The EDX line scanning is performed across the α_3 particle for composition determination. The result shows that besides Al, no other elements are obviously detected in the particle.

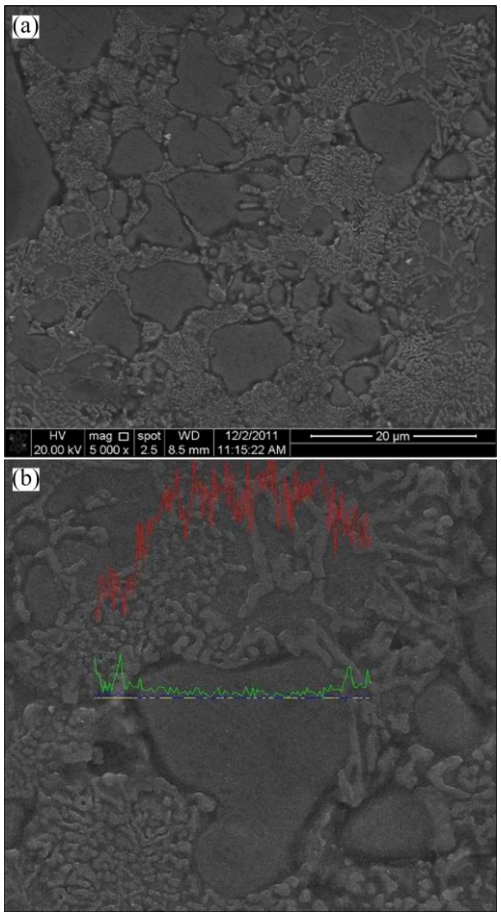

Fig. 8 Rheo-diecasting SEM image (a) and EDX line-scan (b) of ADC12 alloy

3.3 Tensile properties

The tensile properties of rheo-casting ADC12 alloys are presented in Fig. 9. It is observed that the yield strength (YS) and ultimate tensile strength (UTS) of the alloy increase variably at different pouring temperature, but the EL remains nearly constant after rheo-processing. The YS and UTS increase with the decrease of the pouring temperature, and reach the maximum in the range of 580 to 600 °C. At pouring temperature of 580 °C, the UTS and EL of the alloy are 211.0 MPa and 1.9%, respectively, which exhibits the best tensile

property and plastic deformability. While poured at 620 °C, the alloy's UTS reduces to 185.8 MPa, which is nearly the same as that of the unstirred one. The mechanical properties of Al−Si series alloy are closely related to dendrite width of the primary Al, the morphology and size of the brittle eutectic Si phases. By phase analysis (shown in Fig. 4), changes of the eutectic Si from acicular to flake-like should lead to the inferior responses of the property due to its brittle nature. However, the increment of properties implies that the primary phase seems to have played more important roles.

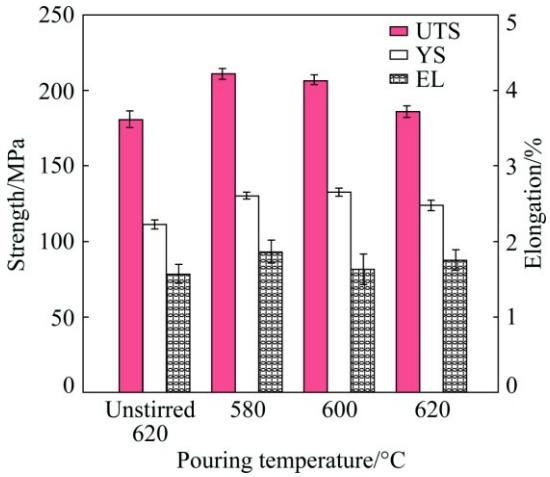

Fig. 9 Tensile properties of liquid casting and rheo-casting ADC12 alloy

Figure 10 shows the tensile properties of HPDC and RDC ADC12 alloys. Compared with the rheo-casting ADC12 alloy (shown in Fig. 9), the tensile properties of the RDC alloy are superior. In Fig.10, it is observed that at the pouring temperature ranging from 595 to 605 °C, the RDC alloy exhibits better tensile properties. At pouring temperature of 595 °C, the alloy obtains the best UTS and EL, which are 276.0 MPa and 4.8%, respectively.

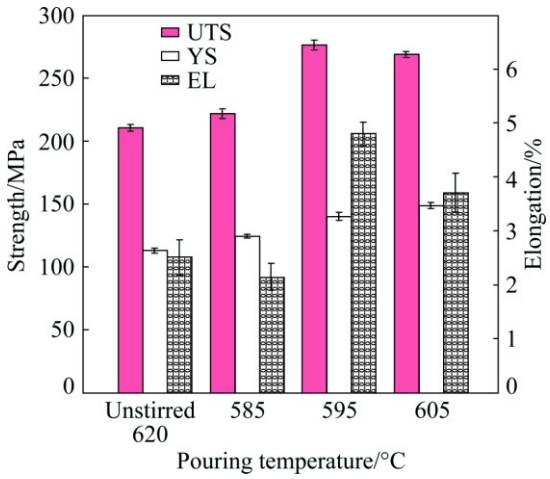

Fig. 10 Tensile properties of HPDC and rheo-diecasting ADC12 alloy

The typical SEM fracture surfaces of the liquid casting and rheo-casting ADC12 alloys are shown in Fig. 11. It is clear that the liquid casting sample has a smooth surface and some large scale tearing ridges could be observed (Fig. 11(a)), suggesting that the fracture characteristic is quasi-cleavage fracture. As the matrix, aluminum is a ductile phase that bears most of the pressures and deforms gradually as the tension goes on. The Si is a hard and brittle strengthening phase, and usually disperses in the neighboring area of the primary dendrite Al. When alloy suffers outer tension, the load-bearing component, i.e., the dendrite Al deforms heavily and then the shearing stress increases gradually to reach the strength limit of the brittle acicular-like eutectic Si. Eventually, this leads to particle breakage and then generates cracks in the deformed areas. As the outer tension goes on, the cracks propagate along the eutectic Si and then lead to large primary Al cleavages and flat planes on the fractured surface. The rheo-casting sample has similar quasi-cleavage surface, but it is rougher, and the cleavage planes are smaller (shown in Fig. 11(b)). It should be noted that the primary Al phase transformed from dendritic to near globular or

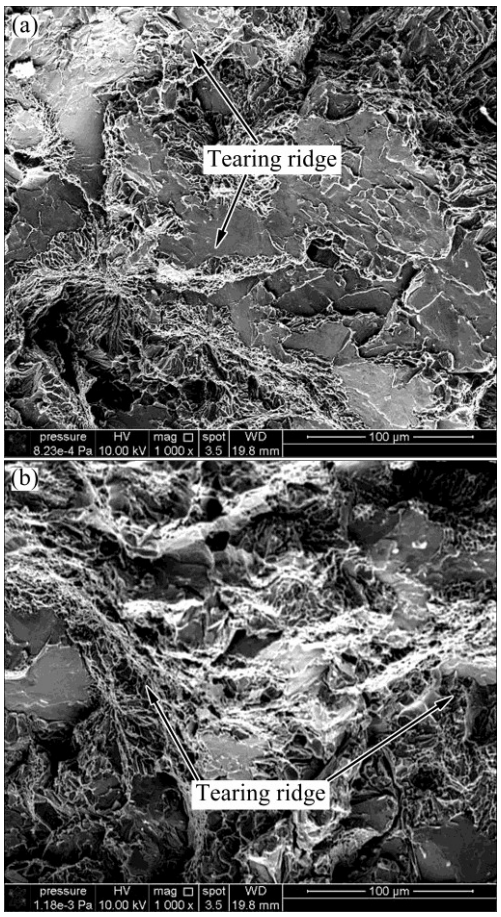

Fig. 11 Typical SEM fractographs of permanent mold casting ADC12 alloy: (a) Liquid casting; (b) Rheo-casting

rosette-like shape (shown in Fig. 4), and the smaller cleavage plane is believed ascribing to the shearing-off of the dendritic primary Al phase.

Figure 12 presents the typical fracture surfaces of the HPDC and rheo-diecasting ADC12 alloys. From a low magnification view, the HPDC sample has obvious large sharp fractural ridges convex from the matrix, indicating that it is where the cracks originated from (shown in Fig. 12(a)). More specific details of the ridges could be observed by larger magnification (shown as Fig. 12(b)). Some severely deformed structures with minor spallings are found, but most of the surfaces are covered by rodlike intergranular cleavages. Fracture surface of RDC sample is greatly different from that of the conventional HPDC, and it is relatively rough, and mainly composed of extensively uniform protrusions with small pits (shown in Fig. 12(c)). The sizes of the protrusions as presented in Fig. 12(d) are 30−50 μm, and with globular or elliptical shapes. The neighboring areas of the protrusions are globular intergranular cleavages which are as large as 10 μm. Combined with the former microstructure analysis (shown in Figs. 6 and 8), characteristics of the protrusions and cleavages are close to α_1 and α_3, suggesting that morphology evolution of the primary Al from dendrite to globular is the key factor to the strengthening of the alloy.

4 Discussion

So far, researches on semisolid processing of ADC12 alloy are limited. WANG et al [7,13] used the strain-induced melt activation (SIMA) process to prepare globular primary Al ADC12 alloy, and a series of isothermal treatments were carried out from 540 to 565 °C. During isothermal treatment, melting occurred in the low melting phase and the high-energy region, and the primary Al morphology evolved from rosette-like to spherical under the driving force of interfacial energy reduction between the solid and liquid phases following the Lifshitz−Slyozov−Wagner theory and Ostwald ripening. It should be noted that the treating temperature is always below the Al−Si eutectic point, and the primary Al inevitably coarsened by a long time of isothermal treatment. JANUDOM et al [8] employed the gas-induced semisolid (GISS) technique to prepare the ADC12 semisolid slurry. The processing temperature was set at 590 °C, and the incorporation of fine gas bubble sheared and fragmented the dendrite by localized cooling and high convection, resulting in grain multiplication. According to the previous literatures analyses, it is noticeable that processing temperatures by SIMA and GISS are different, implying that processing

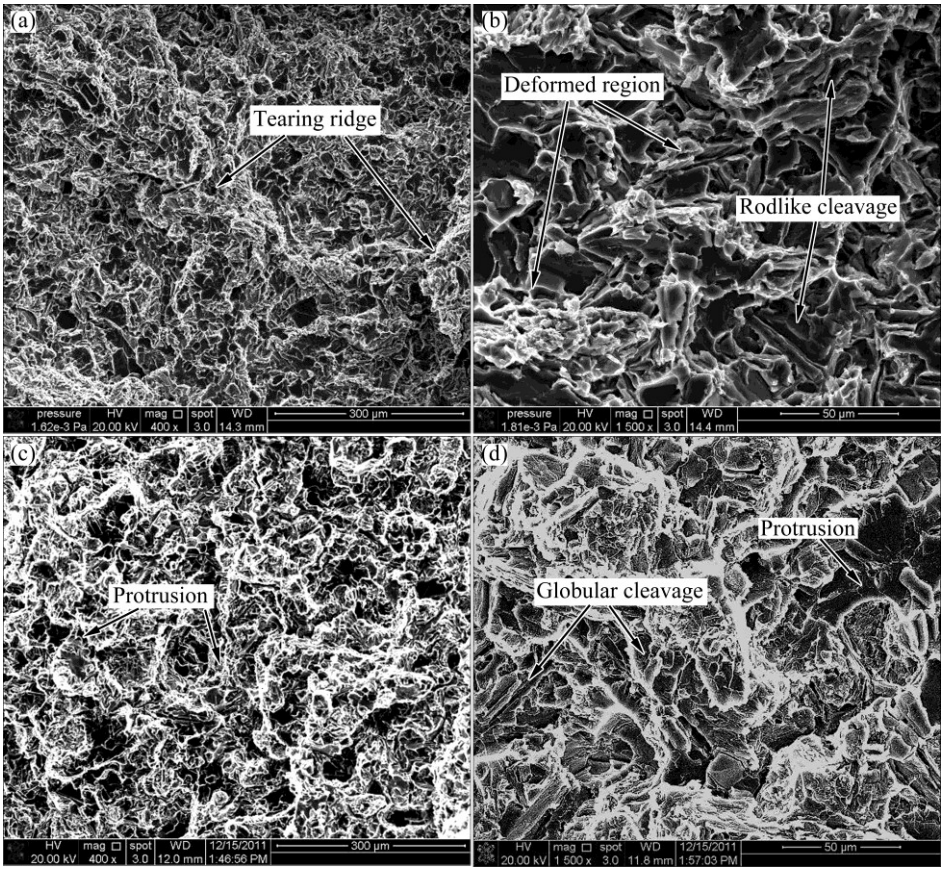

Fig. 12 Typical SEM fractographs of HPDC and rheo-diecasting ADC12 alloys: (a) HPDC; (b) Higher magnification fractograph of HPDC; (c) Rheo-diecasting; (d) Higher magnification fractograph of rheo-diecasting

temperature is a key factor to the successful semisolid processing.

In this work, the MRB process is a dynamic rapid−solidification process, and it appears different mechanisms (shown in Fig. 13) for the formation of globular primary phase compared to isothermal treatment and GISS. For one thing, once the alloy melt with certain superheat is poured into barrel, the rapid barrel rotations can supply large ever-renewing surfaces, leading to the melt chilling which is beneficial to the nucleation. The contact area is usually called “impact zone”, and considered to be the principle source of the nucleation [14,15]. For another, alloy melt flowed along the barrel with continuous cooling, large amounts of the nuclei can form easily on the barrel surface in a heterogeneous way. If the melt solidified in the stable surface, the nucleus will grow along the barrel in dendritic pattern and finally form a solidified layer. However, with rapid rotation, strong vertical stress is applied to the melt, and this can efficiently activate the inhibited nuclei to be active. Similar hypothesis is also confirmed in other semisolid tests. HUANG [16] proved that vibration can break the solid shell formed on the solid surface, and by mould rotation, the chilling solid formed at the wall of mould are detached. Therefore, similar to GISS, the nuclei may break away from the barrel surface and multiplication happens. Thirdly, latent heat could be removed by the relatively cool ever-renewing surface, effectively preventing the recoalescence. Meanwhile, the solute and temperature fields in the melt are prone to be homogeneous under rapid rotation, which restrains the coarsely growing of further primary Al.

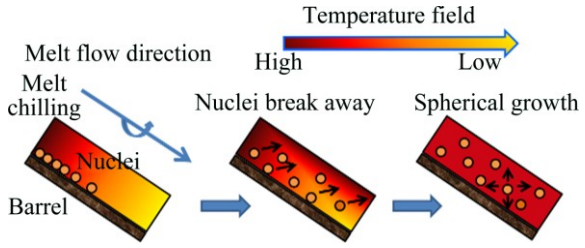

Fig. 13 Schematic diagram of globular primary phase evolution in MRB system

Normally, in the field of semisolid processing, for example, the cooling slope, it is well recognized that casting with low superheat is an effective way to increase nucleation, which is beneficial to a small size of primary phase [6,15]. Non-equilibrium solidification calculation by Scheil model shows that the initial solidification temperature of ADC12 alloy is about 590 °C (Fig. 14). The rotational barrel is effective in removing the superheat, and higher cooling rate is obtained with higher pouring temperature (Tables 2 and 3). The timing for Al−Si binary eutectic reaction depends on pouring temperature, and the eutectic reaction usually happens while alloy melt flows along the barrel at low pouring temperature. The latent heat released by the reaction may lead to recalescence and inhibite nucleation. Furthermore, slow cooling rate results in coarse flake-like Al−Si eutectic microstructure (Fig. 4(d)). Therefore, pouring temperature with low superheat over 590 °C is favorable for the rheo-processing of ADC12 alloy, and the present results show that it does obtain finer primary Al (shown in Figs. 4 and 6).

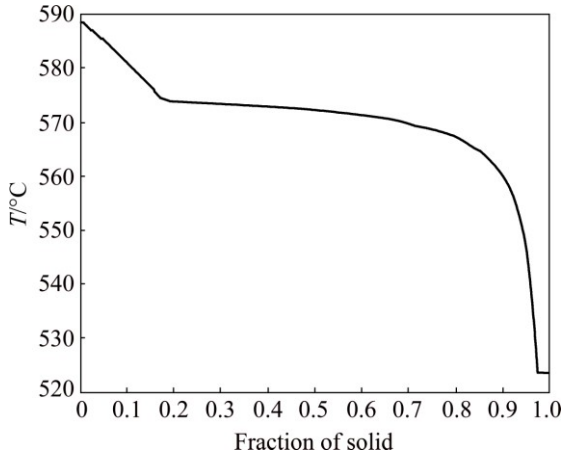

Fig. 14 Fraction of solid vs temperature curve of ADC12 alloy calculated by Pandat software

It is clear from Figs. 9 and 10 that the yield strength, tensile strength and elongation are increased to some extent after rheo-processing by both casting means. By understanding the strengthening mechanisms of the rheo-processed ADC12 alloy, a relationship between microstructure, mechanical properties and processing parameters can be made.

Solid solution and age hardening are well known as key techniques to strengthen and harden Al−Si alloys by Mg and Cu elements going either substitutional or interstitial into and then precipitate homogeneously from the matrix which distorts the crystal lattice and hinders dislocation mobility [17−19]. As illustrated in Fig. 3, only the XRD reflections of the Al slightly shift towards to the higher degree, and no obvious Si and Al_2Cu shifts are observed in the as-cast samples. Further SEM observations and EDX line-scan results confirm that the Al_2Cu does not dissolve in the matrix, while it mainly exists in the Al−Si eutectic district. Therefore, it is understood that the minor elements, for example Cu and Mg, do not contribute much to the alloy strengthening.

In the polycrystalline metal, the mechanical properties are influenced by the size of the grains, and their relationships are usually expressed in terms of the Hall−Petch equation:

$$\sigma_{0.2} = Kd^{-0.5} + \sigma_0 \quad (1)$$

where $\sigma_{0.2}$ is the yield strength, d is the average diameter of the grains, and σ_0 and K are constants for the metal. Some researchers have reported the influence of secondary dendritic arm spacing (SDAS) on the tensile properties of Al−Si alloy, and the Hall−Petch relationships are obtained in the works of OSÓRIO et al [20] and OKAYASU et al [21], where the relationships for ADC10 and ADC12 alloys are $\sigma_{0.2}=6.6d^{-0.5}+40.1$, $\sigma_{0.2}=6.1d^{-0.5}+48.5$, respectively. OSÓRIO et al [20] suggested that the size reduction of SDAS leading to cleaner and sounder cast structure are responsible for the increase in tensile strength. OKAYASU et al [21] attributed the strengthening of ADC12 alloy produced by permanent mould casting (PMC) to the high dislocation density generated from the grains colony which was united by several grains with high misorientation angle, but similar results were not observed in the HPDC sample. OKAYASU et al [21] agreed with that the excellent tensile properties of the alloy were due to the fine round primary Al and tiny eutectic structures, however, the macro defects induced by various casting means, for example shrinkage and porosity, are not discussed.

In this work, tensile properties of the traditional PMC and HPDC are close but those after rheo-processing are superior to Okayasu's work. Figure 15 represents the relationships between the yield stress and primary Al grain size (d) for the RC and RDC samples. Although there are few experimental data, the Hall−Petch relationships of the rheo-processed ADC12 alloy are clearly observed, which are $\sigma_{0.2}=171.2d^{-0.5}+97.3$ (RC) and $\sigma_{0.2}=714.4d^{-0.5}+4.3$ (RDC). The relationships are greatly different from the conventional ADC10 and ADC12 alloys, although they have similar chemical compositions. Substantial efforts have approved that strength and ductility of the cast aluminum alloy are improved after semisolid processing, and the improvement could be attributed to two factors: one is reduction on porosity and the other is microstructure refinement along with composition homogeneity [22]. It is well known that the existence of large pores caused by entrapped gas and shrinkage during dendrite solidification reduces the alloys' mechanical properties. The dendrite being sheared off by rheo-processing during solidification below the liquids temperature improves the rheology of alloy melt, which would be more advantageous for the liquidus penetration for forming, and lead to lower gas entrapment as well as less porosity [23−25]. By numerical analysis, it is understood that the mechanical properties of the ADC12 alloy are severely worsened once the porosity is more than the critical porosity fraction of 3.2% [4]. Figure 16 shows the porosity of ADC12 alloy in different processing conditions. The results clearly show that much less gas

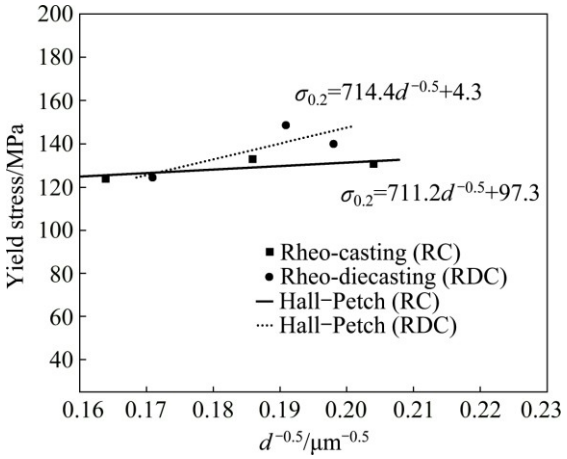

Fig. 15 Relationships between yield stress and primary Al grain size (d) for RC and RDC samples

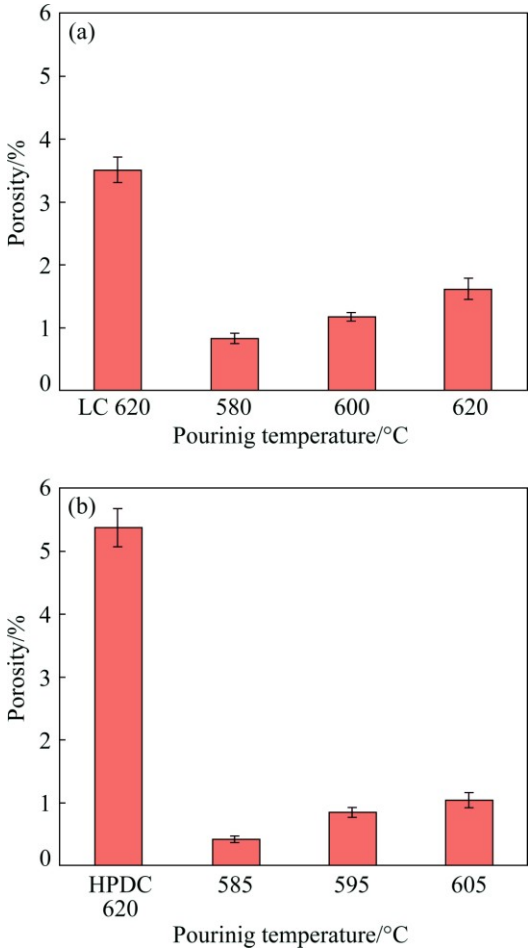

Fig. 16 Porosity of samples under different processing conditions: (a) Rheo-casting; (b) Rheo-diecasting

entrapments are obtained after rheo-processing, which are all below the critical porosity fraction, and similar findings are also observed in another rheo-processed ADC12 alloy by GISS [8]. Similar to OSÓRIO and other semisolid processing literature [22], the great reduction on porosity is considered to be one main factor that

results in the improvement on mechanical properties of semisolid casting ADC12 alloy. On the other hand, under stress, the relatively fine and uniformly distributed globular primary Al obtained by rheo-processing would be in favorable of promoting uniform deformation or even diminishing the stress points around the grain boundary, which further improves the mechanical properties. It should be mentioned that superior fractural characteristics are observed in the RC and RDC samples (Figs. 11 and 12), and these are also believed to be the direct results of the shearing-off of the primary Al as discussed in Section 3.3.

5 Conclusions

1) All the rheo-casting and rheo-diecasting samples are mainly composed of Al, Si and Al_2Cu phases, and no remarkable homogeneity is observed according to the XRD diffraction patterns.

2) Dendritic primary Al phases of the rheo-casting and rheo-diecasting samples are sheared off after rheo-processing, and they are compositionally homogeneous. The average size and solid fraction of the primary Al increase with descending pouring temperature.

3) Mechanical properties of the ADC12 alloy are improved by rheo-processing. Yield strength and ultimate tensile strength of the rheo-casting samples increase with decreasing pouring temperature, and the better properties are obtained in the range from 580 to 600 °C. The rheo-diecasting sample with pouring temperature of 595 °C obtains the best ultimate tensile strength and elongation, which are 276.0 MPa and 4.8%, respectively.

4) All the rheo-casting and rheo-diecasting samples are brittle fractured. The primary dendrite sheared-off is helpful to the alloy strengthening in rheo-casting sample. The porosity of the rheo-processed sample is much less than the liquid casting and high pressure die casting. The reduction on porosity and primary Al globularization are key factors to the superior mechanical properties. Relationships of the primary Al sizes and yield stress of the rheo-casting and rheo-diecasting samples are depicted with Hall−Petch equation, which are $\sigma_{0.2}=171.2d^{-0.5}+97.3$ and $\sigma_{0.2}=714.4d^{-0.5}+4.3$, respectively.

Acknowledgements

The authors wish to express thanks to the joint PhD. program financially supported by the China Scholarship Council (CSC).

References

[1] DAI H S, LIU X F. Refinement performance and mechanism of an Al−50Si alloy [J]. Materials Characterization, 2008, 59: 1559−1563.

[2] GUPTA M, LING S. Microstructure and mechanical properties of hypo/hyper-eutectic Al−Si alloys synthesized using a near-net shape forming technique [J]. Journal of Alloys and Compounds, 1999, 287: 284−294.

[3] HU Xiao-wu, JIANG Fu-gang, AI Fan-rong, YAN Hong. Effects of rare earth Er additions on microstructure development and mechanical properties of die-cast ADC12 aluminum alloy [J]. Jounal of Alloys and Compunds, 2012, 538: 21−27.

[4] ZHAO H D, WANG F, LI Y Y, XIA W. Experimental and numerical analysis of gas entrapment defects in plate ADC12 die castings [J]. Journal of Materials Processing Technology, 2009, 209: 4537−4542.

[5] FLEMINGS M C. Behavior of metal alloys in the semisolid state [J]. Metallurgical Transaction: B, 1991, 22: 269−293.

[6] CURLE U A, MÖLLER H, WILKINS J D. Shape rheocasting of unmodified Al−Si binary eutectic [J]. Materials Letters, 2011, 65: 1469−1472.

[7] WANG Zhen-yu, JI Ze-sheng, SUN Li-xin, XU Hong-yu. Microstructure of semi-solid ADC12 aluminum alloy adopting new SIMA method [J]. Transactions of Nonferrous Metals Society of China, 2010, 20(S): s744−s748.

[8] JANUDOM S, RATTANOCHAIKUL T, BURAPA R, WISUTMETHANGOON S, WANNASIN J. Feasibility of semi-solid die casting of ADC12 aluminum alloy [J]. Transactions of Nonferrous Metals Society of China, 2010, 20: 1756−1762.

[9] RATTANOCHAIKUL T, JANUDOM S, MEMONGKOL N, WANNASIN J. Development of aluminum rheo-extrusion process using semi-solid slurry at low solid fraction [J]. Transactions of Nonferrous Metals Society of China, 2010, 20: 1763−1768.

[10] HU Zhao-hua, WU Guo-hua, ZHANG Peng, LIU Wen-cai, PANG Song, ZHANG Liang, DING Wen-jiang. Primary phase evolusion of rheo-processed ADC12 aluminum alloy [J]. Transactions of Nonferrous Metals Society of China, 2016, 26: 19−27.

[11] HE C Y, DU Y, CHEN H L, XU H. Experimental investigation and thermodynamic modeling of the Al−Cu−Si system [J]. CALPHAD, 2009, 33: 200−210.

[12] HITCHCOCK M, WANG Y, FAN Z. Secondary solidification behavior of the Al−Si−Mg alloy prepared by the rheo-diecasting process [J]. Acta Materialia, 2007, 55: 1589−1598.

[13] WANG Z, JI Z, HU M, XU H. Evolution of the semi-solid microstructure of ADC12 alloy in a modified SIMA process [J]. Materials Characterization, 2011, 62: 925−930.

[14] LEORETTA E C, ATKINGSON H V, JONES H. Cooling slope casting to obtain thixotropic feedstock I: Observations with a transparent analogue [J]. Journal of Materials Science, 2008, 43: 5448−5455.

[15] LEORETTA E C, ATKINGSON H V, JONES H. Cooling slope casting to obtain thixotropic feedstock II: observations with A356 alloy [J]. Journal of Materials Science, 2008, 43: 5456−5469.

[16] HUANG W D, WANG W L, LIN X, WANG M. In situ observation of SSM microstructure formation during cooling slope casting of an NH_4Cl-H_2O alloy with vibrating the slope [J]. Solid State Phenomena, 2006, 116−117: 193−196.

[17] YAN M, ZHU W Z, CANTOR B. The microstructure of as-melt spun Al−7%Si−0.3%Mg alloy and its variation in continuous heat treatment [J]. Materials Science and Engineering A, 2000, 284: 77−83.

[18] SJOLANDER E and SEIFEDDINE S. The heat treatment of Al−Si−Cu−Mg casting alloys [J]. Journal of Materials Processing Technology, 2010, 210: 1249−1259.

[19] GUPTA M, LAVERNIA E J. Effect of processing on the microstructural variation and heat treatment response of a hypereutectic Al−Si alloy [J]. Journal of Materials Processing Technology, 1995, 54: 261−270.

[20] OSORIO W, GOULART P, GARCIA A, SANTOS G A, NETO C M. Effect of dendritic arm spacing on mechanical properties and corrosion resistance of Al 9 Wt Pct Si and Zn 27 Wt Pct Al alloys [J]. Metallurgical and Materials Transactions A, 2006, 37: 2525−2538.

[21] OKAYASU M, OHKURA Y, TAKEUCHI S, TAKASU S, OHFUJI H, SHIRAISHI T. A study of the mechanical properties of an Al−Si−Cu alloy (ADC12) produced by various casting processes [J]. Materials Science and Engineering A, 2012, 543: 185−192.

[22] FAN Z. Semisolid metal processing [J]. International Materials Reviews, 2002, 47: 49−85.

[23] FAN Z. Development of the rheo-diecasting process for magnesium alloys [J]. Materials Science and Engineering A, 2005, 413−414: 72−78.

[24] FAN Z, FANG X, JI S. Microstructure and mechanical properties of rheo-diecast (RDC) aluminium alloys [J]. Materials Science and Engineering A, 2005, 412: 298−306.

[25] LÜ Shu-lin, WU Shu-sen, ZHU Ze-min, AN Ping, MAO You-wu. Effect of semi-solid processing on microstructure and mechanical properties of 5052 aluminum alloy [J]. Transactions of Nonferrous Metals Society of China, 2010, 20(S): s758−s762.

流变加工对 ADC12 合金显微组织和力学性能的影响

胡钊华，彭 翔，吴国华，程大强，刘文才，张 亮，丁文江

上海交通大学 轻合金精密成型国家工程研究中心与金属基复合材料国家重点实验室，上海 200240

摘 要：通过光学显微镜、X 射线衍射和扫描电镜等表征手段，研究流变加工的 ADC12 合金的显微组织演变和力学性能。结果表明：流变铸造和流变压铸下初生铝树枝晶得到破碎，其平均颗粒尺寸、固相率随浇注温度降低而提高。流变加工有效地提高合金的力学性能。流变铸造条件下，合金抗拉强度随着浇注温度降低而提高，在 580 到 600 °C 之间浇注可以获得较高的力学性能。流变压铸条件下，595 °C 浇注可以获得最佳的抗拉强度和伸长率。流变加工对 ADC12 合金力学性能的提高主要在于实现致密度的提高和初生铝的圆整化。流变铸造和流变压铸工艺下初生铝平均颗粒尺寸与屈服强度可以通过 Hall−Petch 公式描述。

关键词：铝合金；铸造；流变加工；流变铸造；流变压铸；力学性能

(Edited by Yun-bin HE)